DEPARTMENT OF SCIENCE
BUREAU OF METEOROLOGY

TECHNICAL REPORT 3

THE ATMOSPHERIC AEROSOL AND ITS INFLUENCE ON INFRARED RADIATION TRANSFER IN THE LOWER ATMOSPHERE

R.D. Hoy

APRIL 1973

DEPARTMENT OF SCIENCE
BUREAU OF METEOROLOGY

TECHNICAL REPORT 3

THE ATMOSPHERIC AEROSOL AND ITS INFLUENCE ON INFRARED RADIATION TRANSFER IN THE LOWER ATMOSPHERE

R.D. Hoy

AUSTRALIAN GOVERNMENT PUBLISHING SERVICE
CANBERRA, 1973

The "Technical Report" series of publications is designed as a means of circulating to fellow scientists, both within and outside the Bureau, the progress achieved on a problem of meteorological interest when a major phase in the investigation has been completed. This publication is generally not an end product but rather a preliminary stage in the preparation of a scientific paper for publication.

Meteorological "Technical Reports" are intended for both internal and external distribution. The external distribution will depend on the content of the particular Technical Report.

Reference to the Report should be made in the following manner:

Technical Report No 3
65/64 of April 1973. Bur. Met., Australia

CONTENTS

	Page
Abstract	1
Introduction	1
Mie scattering theory	3
Aerosol properties	6
Significance of physical properties in radiation transfer	13
Radiative flux in the atmosphere	25
Discussion	35
Acknowledgments	39
References	39
Appendix I Aerosol volume and mass concentrations	

TABLES

Table 1 The absorption coefficient and the real and imaginary parts of the index of refraction for pure water for various wavelengths

Table 2 Relative humidities for which an aerosol of initial radius of stated composition grows by a factor through condensation of water vapour

Table 3 The ratio of the number of aerosols after growth to the number before growth at a given radius for various values of V and a(f)

Table 4 Flux increases

FIGURES

Fig 1 The Junge aerosol size distribution normalised such that the total particle density between 0.1 and 15 microns radius is constant for various V

Fig 2 Planck black body intensity function $P(\lambda)$ for $T = 28^{o}K$ as a function of wavelength in microns

Fig 3 The extinction, scattering and absorption as a function of radius for a Junge aerosol with index V, as labelled, for various refractive indices

Fig 4 The extinction, scattering and absorption as a function of wavelength for a Junge aerosol with index V, as labelled, for various refractive indices

Fig 5 Liquid water and water vapour absorption coefficients

Fig 6 Absorption by liquid water and water vapour for wavelengths from 8 to 13 microns

THE ATMOSPHERIC AEROSOL AND ITS INFLUENCE ON INFRARED RADIATION TRANSFER IN THE LOWER ATMOSPHERE

R.D. Hoy
Head Office, Bureau of Meteorology, Melbourne

ABSTRACT

The variability of the physical properties of the atmospheric aerosol are reviewed. The effect of this variability on the infrared scattering, absorption and extinction by aerosols with a Junge size distribution is discussed for changing relative humidity. For an aerosol which absorbs and scatters radiation, aerosol radii between 0.1 and 5.0 microns dominate the long-wave radiative properties and absorption is more important than scattering

The accuracy of long-wave flux calculations is discussed and some corrections to the generalised absorption coefficient for water vapour suggested. The radiative flux from aerosols may be included in such calculations by equating the volume of water aerosol to a radiatively equivalent quantity of water vapour. The implications for radiative transfer prior to fog formation and during a subsidence inversion are discussed.

INTRODUCTION

The atmospheric aerosol consists of particles with radii of between 0.001 and 20 microns suspended in the atmosphere. It is present at all altitudes although its greatest concentration occurs in the lowest kilometre of the atmosphere. It has been studied for some time because of its ability to act as nuclei for condensation of water vapour to form fog or cloud particles. Recently however, there has been increased interest in its effects on radiative transfer in the atmosphere, both for solar radiation (short-wave) and for infrared (long-wave) radiation. This study deals with the latter and concentrates on changes in the radiative properties of the air due to aerosols at high relative humidities.

This work was initiated to study changes in long-wave radiation transfer prior to fog formation to be applied to improving fog forecasting. However the techniques and results reviewed apply quite generally to long-wave radiation transfer through optically thin clouds of particles. Some of the literature on fog forecasting will now be considered before discussing the physical properties of aerosols and their radiative effects in more detail.

All fog formation involves the production of a layer of saturated air with resultant condensation of water vapour to form fog droplets. A number of processes may produce saturation of the air and these distinguish several types of fog (Shaw, 1963). The most commonly encountered types are advection and radiation fogs. The former involves the movement (or advection) of warm moist air over a surface whose temperature is below the dewpoint of the advected air. The latter involves cooling of the ground and the surface layer of air by long-wave radiation transfer. The turbulent transport of heat and water vapour in the boundary layer is also significant in the formation and evolution of radiation fog.

The physical processes mentioned are dependent on each other, the synoptic situation and the local geography. The synoptic situation will determine whether fog formation is possible but whether fog actually forms at any given place will depend on the local interaction of the above processes.

Stewart (1955), discussing his experimental studies of fog, notes an increase in radiative cooling rates often occurs before fog forms. He suggests this may be due to increased radiation loss from aerosols which have grown due to the high relative humidities. Funk (1960, 1962) using net radiometers shows these rates may be commonly up to 6°C/hour and show rapid variations with time. Calculated radiative fluxes using radiation charts and measured temperature and water vapour profiles (Funk, 1960) underestimate observed cooling rates and do not show the observed rapid fluctuations with time. This suggests that the increased cooling rates may be caused by aerosol radiative effects. Shaw (1963) and Maine (1963) provide a summary of fog formation theory and fog forecasting techniques as well as a large number of practical studies of the forecasting problem for particular locations. Both Funk (1962) and Stewart (1955) comment on the difficulty of determining whether their observations are representative in space and Stewart comments

particularly on the variability of his measured low level moisture profiles with time (and space) suggesting that advection can never be entirely neglected.

For more reliable radiation fog forecasting, more detailed knowledge of the significant physical processes in the period leading up to fog formation is necessary. The process which will be considered in this paper is the change in radiation transmission through the atmosphere for high relative humidities due to swelling of the atmospheric aerosol. As saturation approaches, those aerosol particles which are hygroscopic absorb water vapour from the air and increase in diameter thus becoming more effective radiation absorbers and scatterers. The observed decrease in visibility, due to the formation of a wet haze, on days when the relative humidity rises above 70% shows that aerosol swelling increases the atmospheric scattering and absorption for the visible region of the spectrum.

This paper discusses the effect of aerosol growth on absorption and scattering of long-wave radiation emitted from or near to the earth's surface. An outline of the Mie theory of scattering is presented below and a discussion of some of the physical and chemical properties of the atmospheric aerosol later. This paper also seeks to establish which size range of particles most affect infrared radiation transfer, which wavelength bands in the infrared region are most affected and how the radiation transfer is altered by particle growth near saturation. It also discusses how aerosol absorption effects may be incorporated into a radiation chart calculation for various routine applications and finally some possible future developments.

These results are part of design studies for field and laboratory experiments to investigate the contribution of aerosol scattering and absorption to fog formation : a greater understanding of the physical principles involved should aid more accurate forecasting of the occurrence of radiation fog.

MIE SCATTERING THEORY

In order to study the effects of atmospheric aerosols and fog droplets on infrared radiation transfer, it is necessary to consider scattering and absorption by particles whose diameter (2r) is of the same order of magnitude as the

wavelength of the incident radiation (λ) *ie*, the size parameter α, where $\alpha = 2\pi r/\lambda$, has a value of approximately 1. Neither the Rayleigh theory of scattering, valid for $\alpha << 1$, nor geometric optics valid for $\alpha >> 1$, can be applied in this case. Instead the exact general theory of scattering and absorption, developed by Mie (1908) and based on electromagnetic theory, must be applied. The Mie theory is true for all values of α but the complexity of calculating the various scattering parameters is such that in practice, the theories of Rayleigh scattering and geometric optics are used when appropriate. The introduction of electronic computers within the last twenty years has enabled the easy summation of the complex terms involved in calculating the Mie coefficients, making the theory readily available for general application.

The full Mie theory is given by van de Hulst (1957) and summaries are given in Goody (1964), Bullrich (1964) and Zdunkowski and Strand (1969). For radiation of wavelength λ, incident on a particle of radius r with complex index of refraction $m = n_r - in_i$, it is possible to calculate the Mie angular scattering functions $i_1(\theta)$ and $i_2(\theta)$ where θ is the angle between the scattered path and the unscattered path, $i_1(\theta)$ is the intensity of the component with electric vector normal to the plane of observation and $i_2(\theta)$ the intensity of the component with electric vector parallel to the plane of observation where the incident intensity equals 1. The total scattered intensity function is thus

$$i(\theta) = \frac{i_1(\theta) + i_2(\theta)}{2} \qquad \ldots 1$$

By integrating $i(\theta)$ over the surface of a sphere it is also possible to calculate the Mie coefficients for extinction Q_e, for scattering Q_s and hence for absorption Q_a using the relation $Q_a = Q_e - Q_s$. For a particle of radius r, then, the extinction cross section is given by

$$\sigma_e = Q_e \pi r^2 \qquad \ldots 2$$

and similar expressions hold for the absorption and scattering cross-sections.

Calculations of such cross-sections for water spheres are found in Stephens and Gerhardt (1961), Stephens (1961) and in Herman (1962), the latter including many diagrams of Q_e, Q_s and Q_a. Bullrich (1964) has applied Mie theory to the study of the angular scattering and polerisation properties of the atmospheric aerosol for solar radiation. The angular scattering functions for visible and infrared radiation incident on water spheres with a size distribution as determined by Best (1951) for fog are discussed by Zdunkowski and Strand (1969). A number of papers have been written presenting schemes employing the angular scattering patterns for determination of particle size and other parameters *eg*, Harris (1969) but the problem of determining the size distribution of an aerosol sample can only be solved if certain restrictions are placed on possible distributions with associated loss of resolution, (see Bakhtiyarov, Foitzik, Perelman and Shifrin (1966), Twomey and Howell (1967) and Yamamoto and Tanaka (1969)).

No precise calculations have been included in this study to estimate possible effects on radiation transfer of the strong angular dependence of the Mie scattering. Qualitatively however, most of the long wave radiation from the ground is forward scattered within 30^{o} of its original path and is transmitted through the lower atmosphere, contributing to the long-wave radiative cooling of the earth's surface. Absorption by aerosols tends to slow the rate of cooling of the ground because, on reradiating the absorbed radiation, a proportion is returned to the ground. Any change in the size distribution of the aerosol because of condensation as saturation is approached will affect the rate of cooling of the ground and thus the rate of formation of fog.

Throughout this work single scattering has been assumed since the primary interest is in the period prior to fog formation before the particles form a visible cloud. For considerations of radiation transfer within a well formed fog it would be necessary to include the effects of multiple scattering (Zdunkowski and Korb, 1970) but these will not be considered in this paper.

AEROSOL PROPERTIES

Size Distribution

The range of radii of the atmospheric aerosol is from about 0.001 to 20 microns. Aerosols which have only recently been released into the atmosphere may have a broader range of radii than aerosols of older origin since particles of radius larger than 20 microns tend to settle out under the influence of gravity and those of radius less than 0.05 microns tend to coagulate. This latter effect produces a maximum in the size distribution near 0.1 microns.

Junge (1958) found that the size distribution for natural aerosols in the radius range 0.1 to 10 microns can be represented by

$$dn(r) = cr^{-V}\, d\log r \quad (cm^{-3})$$

$$= 0.434\ cr^{-(V+1)} dr \qquad \ldots 3$$

where dn(r) is the number of particles in the radius interval r to (r + dr), c is a constant depending on the particle density and the exponent V has an experimentally determined value between 2.5 and 4 (see Fig 1). The value of V = 3 is considered to be the typical value for practical applications.

The size distribution of the natural aerosol may be considered as a background common to all the atmosphere at a given altitude. Aerosol size distributions from local sources such as industrial towns, the sea shore or forest fires are superimposed on this background and contribute to the observed variations in aerosol size distributions. (Junge, 1963).

Chemical Composition

The chemical composition of the aerosol is difficult to determine because of the small mass available for analysis. Samples may be collected by filtering large volumes of air, by impaction of a jet of air containing the aerosols onto a surface, usually a glass slide, or by analysis of salts found in rain water. The following ions have been found SO_4^{2-}, Cl^-, NO_3^-, NO_2^-, NH_4^+, Na^+, Mg^{2+}, Ca^{2+}, K^+ but the combinations are not well established. Sodium chloride particles with radii greater than 0.5 microns are certainly present in maritime air but there

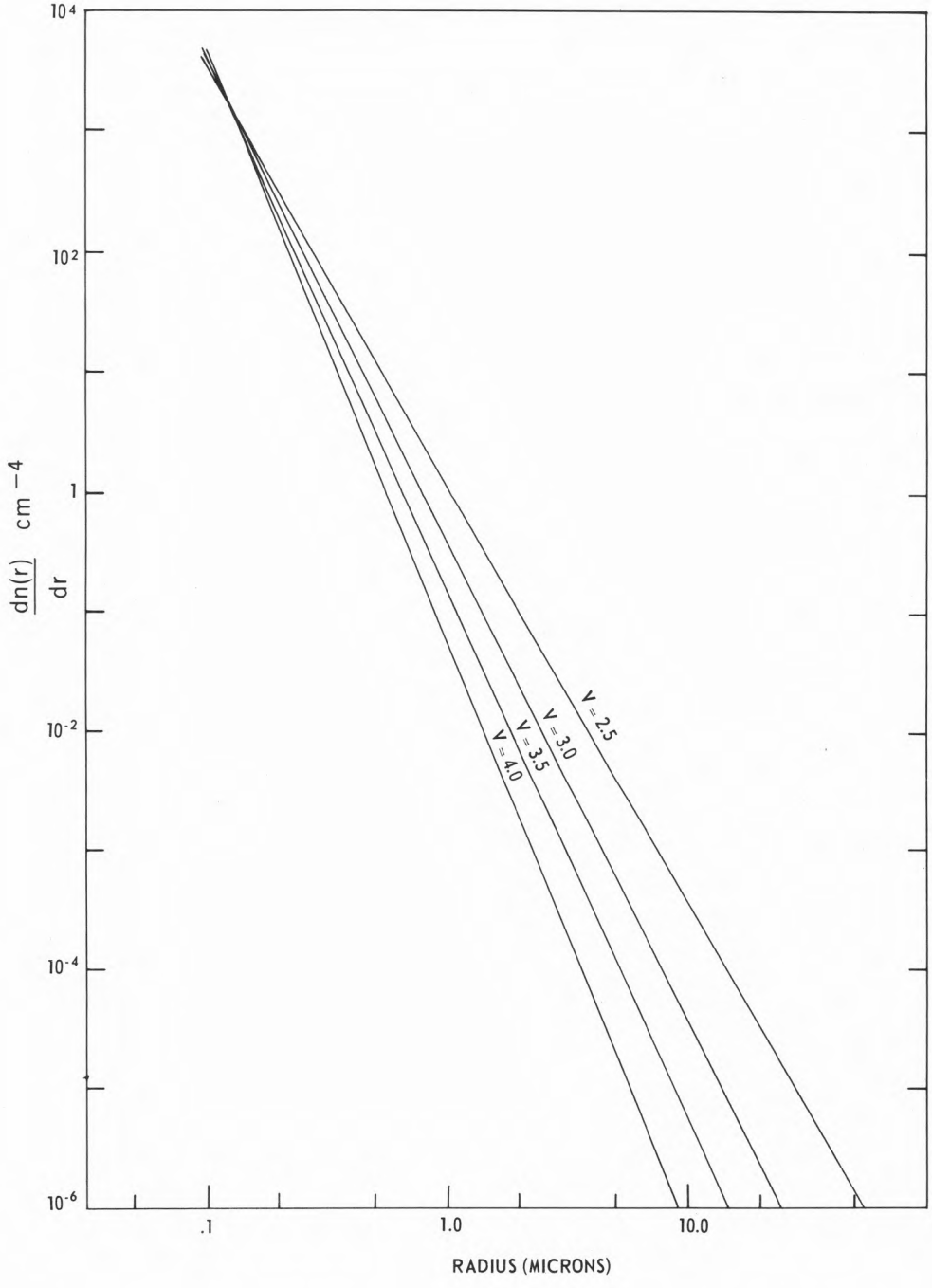

Fig 1 The Junge aerosol size distribution normalised such that the total particle density between 0.1 and 15 microns radius is constant for various V.

is doubt about whether they are a major constituent over the land where ammonium sulphate seems more likely (Twomey, 1971 and Heard and Wiffen, 1969).

Condensation on Aerosols

The atmospheric aerosol is important in fog and cloud studies as it provides a surface on which condensation may occur. Condensation of water vapour in an atmosphere without aerosols would require a saturation ratio of greater than 4 *ie*, a relative humidity of greater than 400% (Fletcher, 1962). Such high saturation ratios do not occur in nature as there is an abundance of aerosols which act as condensation nuclei at relative humidities near 100%.

Condensation may occur before the atmosphere is saturated if a surface is available with certain properties as discussed in detail by Fletcher (1962). A small contact angle between water and the surface lowers the free energy required and condensation may proceed more rapidly. Decreasing the radius of curvature of the surface lowers the vapour pressure at which condensation may take place. If the surface consists of soluble material, formation of a salt solution further lowers the vapour pressure at which condensation may occur. For the natural aerosol consisting of soluble and insoluble materials with condensed water vapour, all these effects are present simultaneously. The relative humidity at which condensation will occur for insoluble particles is determined by the contact angle between water and the surface material, and by the radius of curvature of the surface. Irregularities in the surface in the form of cracks or pores may provide regions of small radius of curvature where some condensation will occur in almost dry conditions (Winkler, 1968). For soluble aerosols a more rapid growth begins when the aerosol will just form a saturated solution in the condensed water vapour. For example sodium chloride particles form a saturated solution near a relative humidity of 75%, ammonium sulphate at about 80% and magnesium chloride near 30%. The growth of soluble material is much more rapid than for insoluble material at high humidities and so only the former is usually considered in theoretical treatments of aerosol growth.

When the atmosphere becomes supersaturated the smaller drops will continue to grow as before. However those larger drops whose critical supersaturation has been exceeded will now continue to grow until all the available water vapour

has been condensed or the drops fall out under gravity. This is the situation in a mature fog or cloud and is discussed in some detail in Fletcher (1962). It will not be further discussed here as it is not of interest for this study.

It should be noted that for decreasing relative humidities supersaturation of the salt solution itself has been commonly observed. Crystallisation of sodium chloride has been observed at relative humidities as low as 40%. However this effect is not well understood and has not been considered in this study.

Dufour and Defay (1964) give the following relation between humidity fraction (relative humidity expressed as a fraction) f and the droplet radius r

$$\ln f \doteqdot \frac{K_1}{r} - \frac{K_2}{r^3} \qquad \ldots 4$$

where K_1 and K_2 are factors dependent on the chemical properties of the salt. The expression is accurate except where the salt solution in the droplet is very concentrated.

Most natural aerosols are considered to be a mixture of soluble and insoluble material and the expression analagous to equation 4 is

$$\ln f \doteqdot \frac{K_1}{r} - \frac{K_2}{r^3 - r_i^3} \qquad \ldots 5$$

where r_i is the radius of the insoluble core, assumed spherical, r is the droplet radius and K_1 and K_2 refer to the properties of the soluble material only.

Use of equations 4 and 5 to study aerosol growth, requires a knowledge of the chemical composition of the soluble material about which agreement has not been reached. Therefore in the preliminary calculations of particle growth with increasing humidity, some experimental data determined by Winkler (1969) and quoted by Kasten (1969), will be used. By weighing many samples of aerosol particles in an environment where the humidity was accurately known, Winkler derived the following law for relative humidities up to 95%

$$\frac{r(f)}{r(o)} = (1 - f)^{-\frac{1}{\mu}} \qquad \ldots 6$$

where r(f) is the aerosol radius for humidity fraction, f and r(o) the radius of the dry particle. The constant μ was determined for each sample by a least squares technique. Its value ranged from 5.8 for a continental aerosol to 3.9 for a maritime sample with a mean over the 28 samples considered of 4.0, the value which has been used in this study. Equation (6) shows the ratio $\frac{r(f)}{r(o)}$ is independent of r(o) (within experimental error) for relative humidities less than 95%. This had already been noted by Junge (1963) and others based on previous experimental and theoretical results.

Refractive Index of Aerosols

To study the transfer of infrared radiation through water or aerosol clouds, it is necessary to know the complex index of refraction $m = n_r - i\, n_i$, for the particles. The real part of m, that is n_r, is the usual refractive index for the material. The imaginary part n_i is a measure of the absorption by the substance at a given wavelength λ and may be determined experimentally by considering the change in intensity of radiation following transmission through a slab of the material of thickness x. If Io is the incident intensity, I the transmitted intensity and R the fraction of intensity reflected, then

$$I = (1-R)\ Io \exp(-kx) \qquad \ldots 7$$

where the absorption coefficient $k = 4\pi n_i/\lambda$ (cm^{-1}). If R = 0, we obtain Beer's Law

$$I = Io \exp(-kx) \qquad \ldots 8$$

Detailed values of the complex index of refraction for liquid water in the infrared are given in the review by Irvine and Pollack (1968) and a few typical values are presented in Table 1 to show the magnitudes expected for different wavelengths.

Table 1 The absorption coefficient (k_v) and the real (n_r) and imaginary (n_i) parts of the index of refraction for pure water for various wavelengths (λ), after Irvine and Pollack (1968)

λ (microns)	n_r	k_v	n_i
0.5	1.336	2.5×10^{-4}	8×10^{-10}
2.0	1.304	68	0.001082
6.0	1.313	2138	0.10208
8.0	1.293	566	0.03603
10.0	1.214	668	0.05316
12.0	1.160	2191	0.2092
15.0	1.330	3601	0.4298
20.0	1.722	2450	0.3899
40.0	1.577	1194	0.3801
60.0	1.670	1245	0.5945

Previous studies of aerosol radiative effects have been concerned mostly with scattering of visible radiation (wavelengths between 0.3 and 0.8 microns) by water spheres for which the absorptive component of refractive index (n_i) is usually assumed negligible. When the effects of dry aerosols are considered, we need to know both n_r and n_i as there is some evidence of absorption even for visible wavelengths. The various combinations of ions previously mentioned give salts with n_r in the range 1.48 to 1.64. A value often used for the real component of refractive index (n_r) of the dry aerosol is 1.55 (Bullrich, 1964). A recent determination of n_r for a number of samples of natural aerosols gave the range 1.50 to 1.63 with a mean value of 1.57 for a relative humidity of 40% (Hanel, 1968). Eiden (1966), from studies of the elliptical polarisation of light, obtained values of n_i for dry aerosols of 0.01 and 0.065 for wavelengths of 0.45 and 0.65 microns respectively. Since n_i for water increases from the visible into the infrared region (see Table 1), it was assumed that, for the dry aerosol n_i would not decrease and would most prob-

ably increase suggesting an estimate for n_i of 0.1 (Eiden, 1968). This suggests that for visible radiation dry aerosols have a mean refractive index of m = 1.55 - 0.1i.

Volz (1972a) has experimentally determined complex refractive indices for dry aerosol material remaining after evaporation of rain water, snow and ice by measuring sample reflections in an infrared spectrometer for wavelengths from 2.5 to 40 microns. There is considerable variation between different aeorsol samples, however a mean value of n_r = 1.7 and n_i = 0.1 was obtained for wavelengths from 8 to 13 microns. An interesting feature of all samples was a maximum value of n_i of up to 0.3 between 9 and 10 microns, near the centre of the atmospheric window, implying that even the dry aerosol is an active absorber and emitter in this spectral band. For the purposes of later discussion the refractive index of dry aerosols in the infrared is taken to be m = 1.55-0.1i. This may underestimate the contribution of scattering but a later section will show that scattering is of only minor importance compared to absorption for wavelengths near 10 microns. Further measurements of natural aerosol refractive indices are required to verify the results of Volz (1972a,b).

The combustion of organic material will produce large numbers of carbon particles which, when not rapidly dispersed, will alter the mean refractive index of the atmospheric aerosol. Guttler (1952) measured the complex index of refraction of carbon to be m = 1.94-0.66i. Twitty and Weinman (1971) have reviewed measurements of the index of refraction of carbon and have deduced a mean value of m = 1.8-0.5i for wavelengths from 0.25 to 15 microns. The measurements show wide variations in n_i and n_r due partly to the different forms of carbon which may be found in the atmosphere *eg*, graphite, soot or coal dust. Comparison of this value with the value for liquid water in Table 1 shows that carbon particles absorb much more strongly than water spheres at all wavelengths and so may not be neglected in any radiation calculation where they occur in large numbers.

Most aerosol particles consist of some insoluble and soluble material. When the relative humidity is greater than about 70%, the soluble material dissolves to form a shell of liquid about the insoluble component. Guttler (1952) has also studied theoretically the Mie scattering problem for spherical particles consisting of an insoluble core and a liquid coating of variable thickness. He found that the shell

structure has no influence on particle optics if the mixing ratios of the components differ only slightly and also if the radius of the particle is approximately equal to the wavelength of the incident radiation (Bullrich, 1964). This means that the property holds approximately for the range of Mie scattering. Thus it may be assumed that for humidities where the mixing ratio of salt solution is greater than the mixing ratio of solid material in the aerosol, the aerosol acts as a sphere of salt solution and that the effect of the insoluble component is negligible with regard to radiative properties. This property will be useful in a later section.

SIGNIFICANCE OF PHYSICAL PROPERTIES IN RADIATION TRANSFER

Introduction

The physical properties of the atmospheric aerosol and the range of variability of these properties were discussed previously. We will now consider how the radiative properties of an aerosol cloud will be affected by these physical properties and how these effects vary with wavelength and particle radius. This should enable the determination of which physical properties are important for radiative transfer prior to fog formation.

A typical aerosol will thus be considered with a Junge size distribution as in Eq 3. The range of aerosol radii considered is from 0.1 to 15 microns (see Fig 1). The maximum number density of particles occurs at a radius of 0.1 microns. For smaller radii the number density is approximately constant then decreases rapidly due to coagulation. The numbers of particles per unit volume will be constant at 135 per cm^3 while V varies from 2.5 to 4.0. This is achieved by letting

$$c = \frac{V \cdot 10^{3-V}}{3} \qquad \ldots 9$$

in Eq 3 (see Appendix). Extinction, absorption and scattering will be calculated from Mie theory, as discussed, which assumes the aerosols are spherical in shape and of a uniform complex refractive index. This is true for water spheres but is only an approximation for irregularly shaped dry or partly wetted aerosols. The refractive indices for water spheres are based

on Irvine and Pollack (1968). The refractive index for dry aerosols will be 1.55-0.1i with some variation in absorptive component. The refractive index of carbon particles was assumed to be 1.94-0.66i.

Dependence of Aerosol Radiative Properties on Radius

To study the dependence of radiation extinction (E) absorption (A) and scattering (S) on aerosol radius, the aerosol cross-sections (for E, A and S) $\pi r^2 Q(r,\lambda)$, weighted according to Planck black body intensity and the Junge aerosol distribution, and integrated over black body wavelengths 6 to 70 microns, were calculated from

$$\sigma(r) = \pi \cdot \log_{10} e \cdot c \cdot r^{1-V} \int_{6}^{70} Q(r,\lambda) P(\lambda) d\lambda \qquad \ldots 10$$

$\sigma(r)$ is the cross-section for extinction, absorption or scattering by particles of radius r, $Q(r,\lambda)$ is the Mie coefficient for extinction, absorption or scattering and $P(\lambda)$ is the Planck intensity function (Goody, 1964) for terrestrial temperatures.

$$P(\lambda) = \frac{X^5}{21.201\ (e^X - 1)} \qquad \ldots 11$$

where $X = 1.43868/\lambda T$. The temperature used was $280^{\circ}K$ (Fig 2) for which 96% of the total radiant energy lies between 6 and 70 microns wavelength. Other non-freezing terrestrial temperatures would give very similar results if used in Eq 10.

The integration of Eq 10 was performed using a combination of Simpson's rule and Newton-Coates 3/8 rule for wavelength increments of 1.0 microns. Comparison with integrals calculated using the Romberg extrapolation method showed good agreement and it is concluded that the results shown are accurate to better than 1%.

The quantity $\sigma(r)/\pi \log_{10} e$ as a function of aerosol radius is shown in Fig 3(a) to (e). $\sigma(r)$ for the simple case of m = 1.55 is shown in Fig 3(a). No absorption takes place and hence extinction equals scattering and only one curve is shown for each V. The aerosols which have greatest influence are those with radius greater than about 1 micron. The order

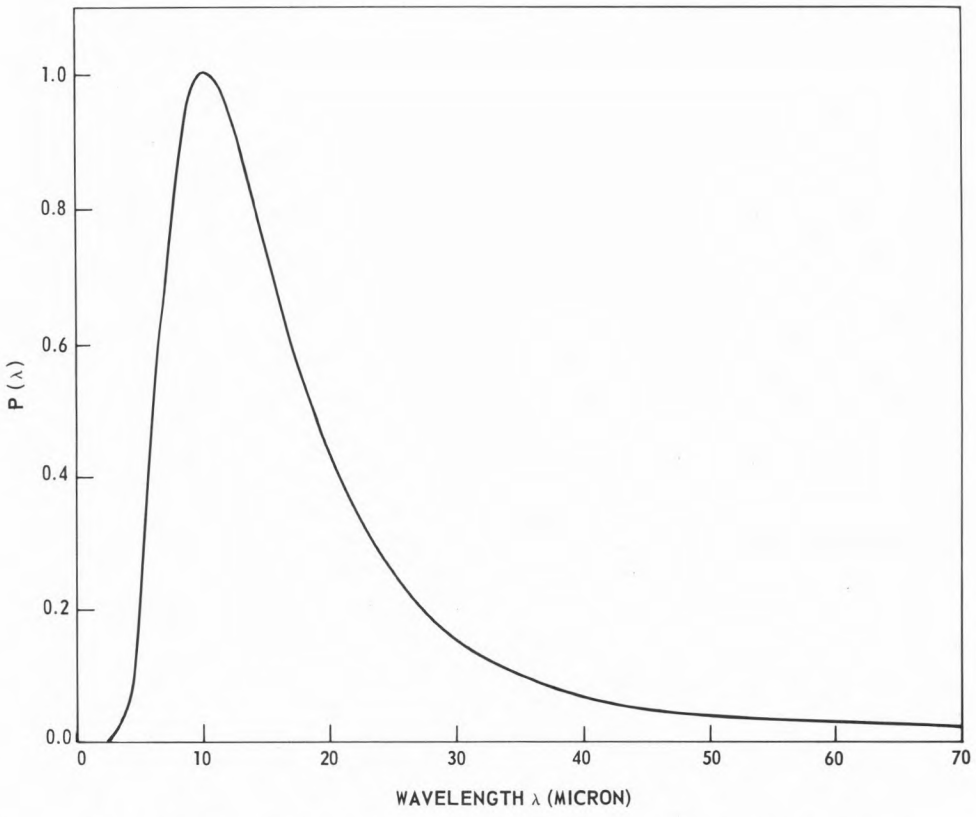

Fig 2 Planck black body intensity function $P(\lambda)$ for $T = 280^{\circ}K$ as a function of wavelength in microns.

of magnitude changes in $\sigma(r)$ for changes in V shows the effect of increasing the numbers of aerosols larger than 1 micron relative to those smaller than 1 micron, remembering that the total aerosol number density for various V is constant.

The effect of increasing the absorption of aerosols is shown in Fig 3(b) and 3(c). The contribution of scattering decreases as absorption increases. Absorption is greatest for particles with radii less than 1 micron. Little change in extinction, as n_i increases for radii greater than 4 microns, is shown in Fig 3(a), (b) and (c). The corresponding curves for carbon particles is shown in Fig 3(d). The further increase in absorption can be seen and an increase in extinction due to

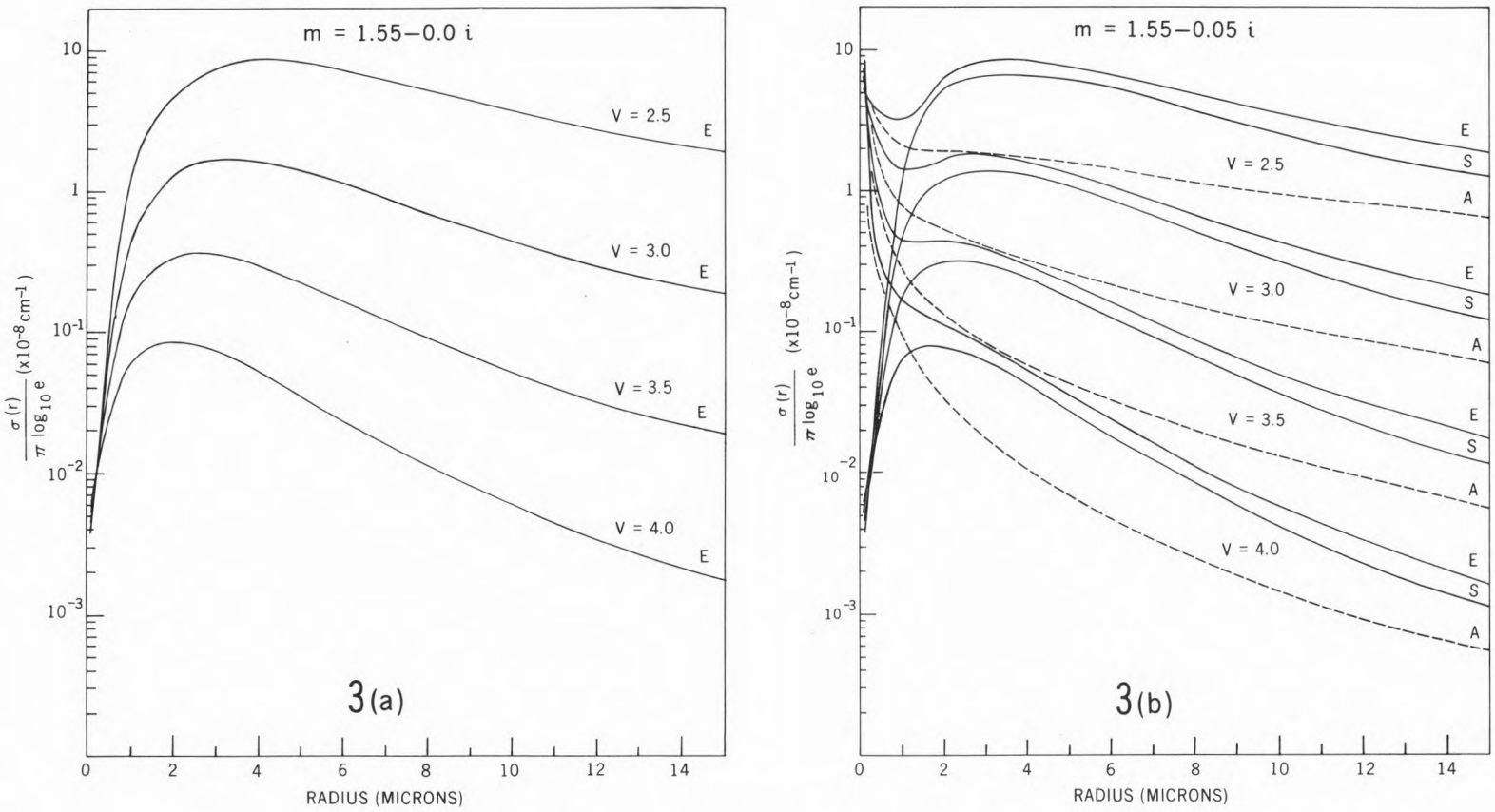

Fig 3 The extinction (E), scattering (S) and absorption (A) as a function of radius for a Junge aerosol with index V, as labelled, for the following refractive indices: (a) m = 1.55–0.0 i, (b) m = 1.55–0.05 i, (c) m = 1.55–0.1 i, (d) m = 1.94–0.66 i and (e) liquid water after Irvine and Pollack (1968).

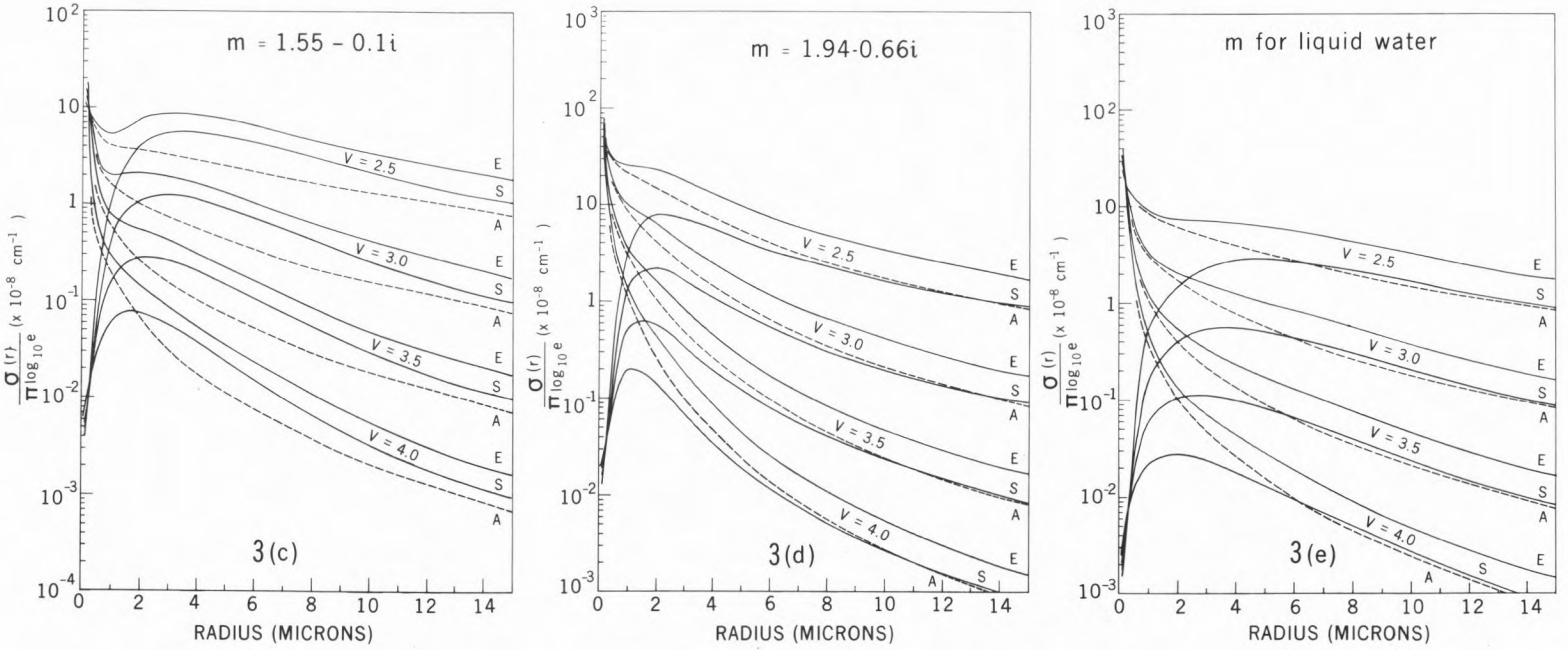

Fig 3 (continued)

increases in both scattering and absorption for radii near 2 microns can be observed. Extinction by water spheres in Fig 3(e) shows no maximum of $\sigma(r)$ near 3 microns radius. Of the five different refractive indices, the extinction due to (d) is greatest followed by (e), (c), (b) and (a).

There exists a strong dependence of $\sigma(r)$ on the index V and on the absorptive component of refractive index n_i for a constant particle number density as shown in Fig 3(a) to (e). The measurement of these quantities is necessary for accurate determinations of aerosol radiative effects. Under conditions where aerosol size may be controlled, absorption dominated processes may be distinguished from scattering dominated processes by the presence of a peak in the $\sigma(r)$ curve below 2 microns. The absence of such a peak suggests scattering is the main process. Quantitative determinations of the absorptive component of refractive index would probably be difficult owing to the effects of index V and real refractive index n_r. In the case of Fig 3(e), $\sigma(r)$ is dominated by particles with radii less than 2.0 microns, thus any study of water sphere radiative effects requires the accurate knowledge of the size distribution of this particle size range. Estimates of aerosol radiative properties can be obtained from total particle counts only if V is measured simultaneously. However, some quantity dependent on size distribution, such as the mass of aerosol material per unit volume, could provide useful estimates of aerosol radiative properties particularly where absorption is predominant.

Dependence of Aerosol Radiative Properties on Wavelength

To determine the wavelengths for which aerosol extinction is greatest, $\pi r^2 Q(r,\lambda) dn(r)/dr$ is calculated for each wavelength and each aerosol radius then integrated over radii from 0.1 to 15 microns.

$$\sigma(\lambda) = c.\log_{10} e.\pi \int_{0.1}^{15} Q(r,\lambda) r^{-V+1} \, dr$$

This equation is evaluated by substituting $\alpha = 2\pi r/\lambda$ and integrating over α from α_1 to α_2 corresponding to radii of 0.1 microns and 15 microns. Thus

$$\sigma(\lambda) = \frac{c \log_{10} e}{4\pi} (2\pi)^V \lambda^{2-V} \int_{\alpha_1}^{\alpha_2} Q(\alpha) \alpha^{1-V} d\alpha \qquad \ldots 12$$

The integration of Eq 12 was performed using a combination of Simpson's rule and Newton-Coates 3/8 rule. Because of the rapid change in the integrand for r < 4 microns, the integration was calculated for increments of 0.1 microns in r from r=0.1 to 4.0 and in increments of 0.5 microns from r=4.0 to 15 microns. Once again comparison with other integral schemes suggests these results are accurate to within 1%.

Curves of $\sigma(\lambda)$ for E, A and S for V=2.5 and V=4.0 V=3.0 and 3.5 were omitted to minimise confusion on the diagrams) for an aerosol with m=1.55-0.1i, typical of the naturally occurring atmospheric aerosol are shown in Fig 4(a). For V=2.5, absorption and scattering change slowly with wavelength and are of similar order of magnitude although scattering predominates slightly at the more important wavelengths less than 35 microns. However as V becomes larger, scattering decreases in importance relative to absorption until at V=4.0, absorption predominates almost completely at all wavelengths. $\sigma(\lambda)$ for E, A and S for V=2.5 and V=4.0 for an aerosol with m=1.94-0.66i, typical of carbon particles is shown in Fig 4(b). Increases in E, A and S occur by comparison with Fig 4(a). For V=2.5, absorption is more important than scattering for all wavelengths, showing the influence of the greatly increased n_i. Once again as V increases, absorption becomes more important than scattering.

The values of refractive index used for Fig 4(a) and (b) are estimated mean values as discussed previously. More detailed determinations of the variability of aerosol refractive indices are required before calculations such as Eq 12 will give results as accurate as those for water spheres. It is also anticipated that refractive indices of naturally occurring and man-made aerosol will show wide variations depending on the source and age of such aerosols. Thus the mean values used above may be considered as the average values of scattering properties about which considerable variation may occur for particular locations.

$\sigma(\lambda)$ for aerosols having the refractive index of water spheres is shown in Fig 4(c). These values reflect the changes in n_i and n_r with wavelength as shown in Table 1 in particular the minimum in absorption near 8.0 microns

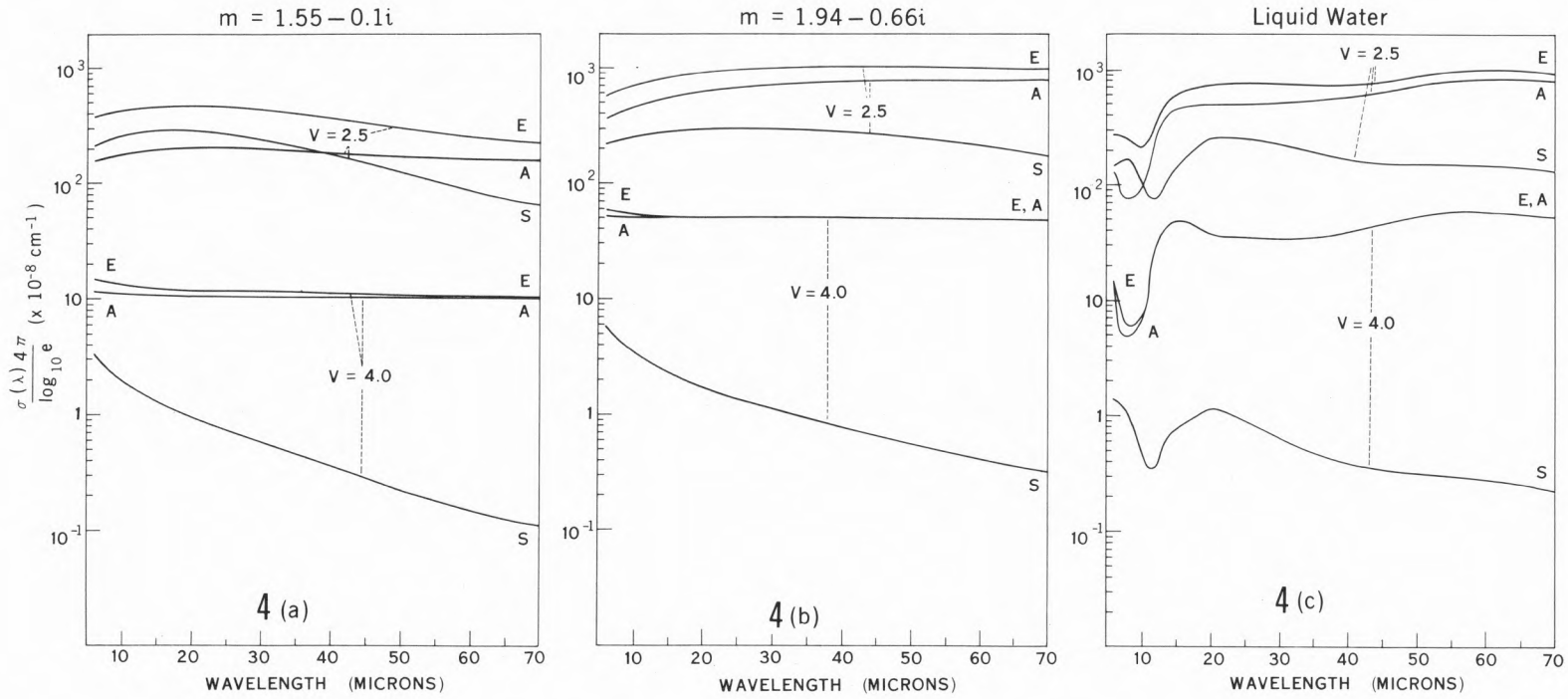

Fig 4 The extinction (E), scattering (S) and absorption (A) as a function of wavelength by a Junge aerosol with index V, as labelled, for refractive indices: (a) m = 1.55-0.1i, (b) m = 1.94-0.66i and (c) liquid water after Irvine and Pollack (1968).

and the minimum in scattering near 12 microns. It is clear that above about 11 microns that the larger part of extinction is caused by the absorptive process for V = 2.5 and as V increases *ie*, the proportion of small aerosols to large aerosols increases, the extinction is principally absorptive in character.

Comparison of Fig 4(a) and 4(c) for extinction for V=2.5 shows that the change from dry natural aerosol to wet natural aerosol of the same size distribution results in an increase in extinction for wavelengths greater than 13 microns but a decrease for wavelengths less than this including the important "atmospheric window" region (8-13 microns). For extinction for V=4.0 an increase in extinction occurs for wavelengths longer than 11 microns, and a decrease for wavelengths shorter than this. In this latter case part of the window region has an increase and part a decrease. Usually the change from dry to wet aerosol is accompanied by a change in size distribution, the aerosols increasing in size as water vapour condenses. The effects of the change in size distribution will be considered below.

Comparison of Fig 4(b) and 4(c) shows that extinction for V=2.5 and 4.0 decreases by changing from carbon particles to water spheres for all wavelengths except beyond 50 microns in the case of V=4.0. Thus carbon particles in the atmospheric window show greater infrared activity than water spheres and could have considerable influence on long-wave cooling rates near industrial areas.

Dependence of Aerosol Radiative Properties on Relative Humidity

As relative humidities increase above 70%, water vapour from the atmosphere will condense on aerosols causing increases in aerosol radius and thus changes in aerosol radiative behaviour. The radius growth for relative humidities up to 95% is given by Eq 6 as a function of humidity, independent of aerosol radius. For relative humidities greater than 95%, the growth of aerosols r(f)/r(o) is a function of radius as well as relative humidity with larger aerosols growing more rapidly than smaller ones. Equation 6 could be used up to 98% relative humidity provided the effects of underestimating the growth of large aerosols is small. The large particles of a Junge distribution do not contribute greatly to the overall radiative properties of aerosols (Fig 3(a) to (e)) and so Eq 6 is probably sufficiently accurate up to 98% relative humidity. Some relative humidities for specified r(f)/r(o) are shown in Table 2,

based on Eq 6 for the mean aerosol and Eq 5 for NaCl. (The results for NaCl were left incomplete owing to theoretical uncertainty in radii at high solution concentrations occurring below 80% relative humidity). The mean aerosol values of Table 2 shown in parentheses would be sufficiently accurate for aerosols less than about 3 microns radius but would be too small for larger aerosol radii.

Table 2 Relative humidities (%) for which an aerosol of initial radius r(o) of stated composition grows by a factor r(f)/r(o) through condensation of water vapour

Radius Growth $\frac{r(f)}{r(o)} = a(f)$	Mean Aerosol	NaCl
1.5	80	-
2.0	94	84
2.5	(98)	91
3.0	(99)	95

Knowing the size distribution of aerosols and the growth law applicable, we may calculate for any particle radius r the increase in particle number density as growth occurs. From Eq 3 a Junge aerosol size distribution has the form

$$dn(r) = n(r)dr$$
$$= Kr^{-(V+1)}dr$$

where dn(r) is the number of aerosols per unit volume in the radius interval r to r+dr and K is a constant. From Eq 6, aerosol growth has the form

$$\frac{r'}{r} = a(f)$$

where r' is the radius at humidity fraction f for a radius of r at relative humidity 0. The size distribution after aerosol growth from r to r' is n'(r').

The number of aerosols is conserved during growth, thus

$$n'(r')dr' = n(r)\,dr$$
$$= n\left(\frac{r'}{a(f)}\right)\frac{dr'}{a(f)}$$
$$= \left[a(f)\right]^{V} n(r')dr' \qquad \ldots 13$$

ie, the ratio of the number of aerosols before and after growth at the same radius is a function of the relative humidity f and the Junge distribution index V. Distributions with large V grow more rapidly than those with small V for the same relative humidity change. Some values of $\left[a(f)\right]^{V}$ are shown in Table 3 for expected values of a(f). The relative humidities for a(f) to occur for a mean aerosol and NaCl may be found in Table 2.

Table 3 The ratio of the number of aerosols after growth to the number before growth at a given radius for various values of V and a(f)

a(f) \ V	2.5	3.0	3.5	4.0
1.5	2.76	3.38	4.14	5.08
2.0	5.66	8.0	11.3	16.0
2.5	9.89	15.6	24.7	39.1
3.0	15.6	27.0	46.8	81.0

The effect of increasing relative humidity in Eq 10 and 12 can now be easily estimated by taking the appropriate $\sigma(r)$ or $\sigma(\lambda)$ before growth and multiplying by the corresponding value in Table 3 appropriate to the parameters V and a(f). For instance for a mean aerosol with V=2.5, m=1.55-0.0i, r=2 microns (Fig 3(a)), $\sigma(r)/\pi\log_{10}e = 47 \times 10^{-8}\,cm^{-2}$. At a relative humidity of 94%, a(f) = 2 and the refractive index is that of water so that from Fig 3(e) and Table 3

$$\sigma(r)/\pi \log_{10} e = 5.66 \times 7.5 \times 10^{-8} \text{ cm}^{-2}$$
$$= 42.5 \times 10^{-8} \text{ cm}^{-2}$$

ie, there is almost an order of magnitude increase in extinction due to aerosols at 2 microns with V=2.5 for a change in environment from dry to 94% relative humidity. An even larger increase would occur for large V or for NaCl aerosol. If the aerosol consisted largely of carbon particles, then, before growth (see Fig 3(d)), $\sigma(r)/\pi \log_{10} e = 23 \times 10^{-8}$ cm^{-2} resulting in a much smaller increase in $\sigma(r)$, assuming the wet aerosols at 95% acted as water spheres.

The effects of water mixtures of various aerosol materials on the refractive index is not easy to estimate as it depends on the solubility of the aerosol. It is assumed here that sufficient water is present to coat the particle so that it behaves as a water sphere. At lower relative humidities this is unlikely to be accurate and so proportional weighting by volume of water and aerosol solid could be used for greater accuracy.

The total extinction, absorption or scattering cross-sections of an aerosol with a given size distribution may be obtained by integrating over r from 0.1 to 15 microns *ie*, by calculating the area under the curves in Fig 3(a) to (e). The effect of a change of relative humidity on these total cross-sections may also be obtained by use of Table 3.

We may conclude that to study aerosol radiative properties and their variation with relative humidity we need to know or estimate the following aerosol physical properties:

the complex refractive index $m = n_r - in_i$ for the infrared wavelengths required

the radius growth law for increasing relative humidity a(f), and

either the size distribution or the number density of particles together with the Junge index V.

RADIATIVE FLUX IN THE ATMOSPHERE

Empirical inclusion of liquid water in flux calculations

Long-wave radiative fluxes in the atmosphere, are influenced by the surface temperature of the earth and the temperature structure and concentrations of atmospheric constituents which are active absorbers and emitters of long-wave radiation at terrestrial temperatures. These include in general solid material *eg*, aerosols or smoke particles, liquid particles in the form of clouds and the various atmospheric gases. The two most common of these naturally occurring gases are carbon dioxide which strongly absorbs between 13 and 17 microns and water vapour which strongly absorbs from 5 to 7 microns and for wavelengths greater than about 20 microns. Ozone has a narrow absorption band at 9.6 microns but its effect will not be considered since ozone does not occur in significant quantities in the lower atmosphere (Pittock, 1968). The atmosphere is relatively transparent to the earth's black body radiation only in a narrow region from 8 to 13 microns which is known as the atmospheric window. At other wavelengths most of the radiation is absorbed by carbon dioxide and water vapour and re-emitted by them at some lower temperature than the surface of the earth. Thus any calculation of radiation flux in the atmosphere must consider the radiation emitted by these two gases as well as that originating at the surface of the earth.

The calculation of these radiation fluxes for various levels in the atmosphere is difficult to perform exactly. It is necessary to know the amount of water vapour present and its temperature in the atmosphere to be able to calculate the radiative flux which it produces. This information is usually given in the form of u', the optical depth of water vapour (corrected for the variation in absorption due to pressure and temperature of the gas) as a function of T, the temperature of the gas. The units of u' for water vapour are given as precipitable centimetres (prec cm) or g cm^{-2}. The downward flux (at a reference level) due to water vapour may then be calculated from:

$$F_w = -\int_o^{\infty} d\lambda \int_o^{u'} F_{\lambda b} \frac{d\,\tau_f}{d\,u'}\, du' \qquad \ldots 14$$

where $F_{\lambda b}$ is the black body flux from a body at wavelength λ, u' is corrected optical depth of water vapour and $\frac{d\tau_f}{du'}$ is the variation in transmissivity with optical depth over a small wavelength interval, and depends on the values of the generalised water vapour absorption coefficient $k_v(\lambda)$ shown in Fig 5. (The generalised absorption coefficient is the result of averaging the absorption spectrum over a finite wavelength interval to smooth out the fine structure of individual lines). In practice it is necessary to use a numerical technique to evaluate Eq 14. The area enclosed by the u', T profile on a special chart is proportional to the flux.

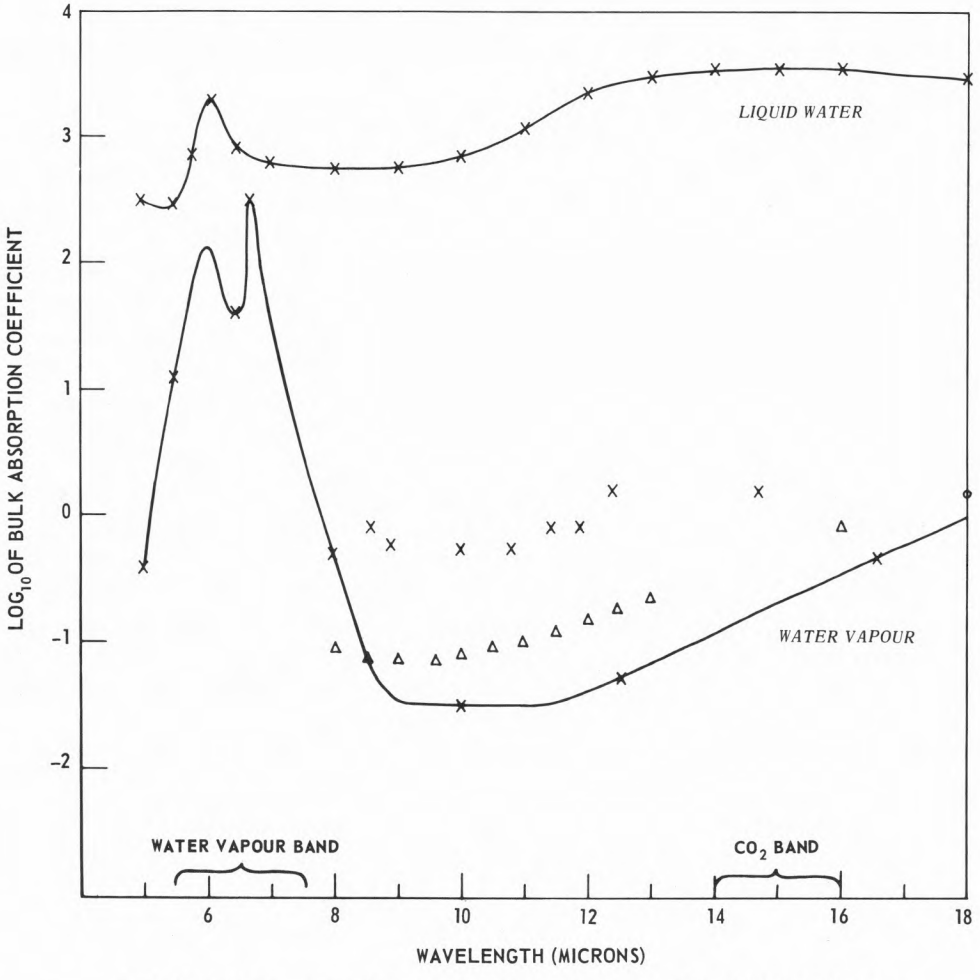

Fig 5 The bulk absorption coefficients for liquid water after Irvine and Pollack (1968) and for water vapour after Elsasser and Culbertson (1960) are shown as solid lines. Crosses (x) are water vapour absorption coefficients used by Myers (1966) and triangles (Δ) are water vapour absorption coefficients measured by Bignell (1970).

The simultaneous calculation of fluxes from water vapour and carbon dioxide is treated differently by different radiation charts. The radiation chart devised by Elsasser (1942) assumed carbon dioxide was completely absorbing for radiation from 13 to 17 microns. Elsasser and Culbertson (1960) have computed transmissivity tables for carbon dioxide in a similar way to water vapour and suggest an approximate method to allow for the overlap between water vapour and carbon dioxide absorption bands. Kondratyev (1969) provides tables to calculate u' for water vapour and carbon dioxide together (allowing for the overlap of bands) to be used with his radiation chart. A number of other radiation charts are available. Kondratyev and Nijlisk (1960) provide a comparison. Thus the radiation fluxes from the earth and the two most common gases in the atmosphere may be calculated for any level in the atmosphere and from these, cooling rates determined from the radiative flux divergence.

A known deficiency of such charts is that they do not consider the effects of solid or liquid material in the atmosphere. The strong absorptivity of carbon particles in the infrared and the weaker absorption due to the natural aerosol have previously been discussed. For relative humidities greater than 70%, many aerosols will act as water spheres which will absorb strongly in the infrared. Carlon (1970) has noted the greatly enhanced absorption and emission which would arise particularly in the window region, if a small quantity of the water vapour in the air should condense on aerosols.

The absorption (%) due to water vapour and liquid water in the 8 to 13 micron window region, calculated using Beer's Law, is shown in Fig 6. The absorption coefficient $k_\ell(\lambda)$ for liquid water is after Irvine and Pollack (1968) and $k_v(\lambda)$ for water vapour after Bignell (1970) (Fig 5). Both Fig 5 and 6 show similarities in the wave-length dependence for absorption by liquid water and water vapour, especially considering the experimental problems of determining $k_v(\lambda)$ for water vapour in the window region. This suggests that an empirical relation between $k_\ell(\lambda)$ and $k_v(\lambda)$ may be derived so that the radiative effect of a quantity of liquid water may be represented by a corresponding quantity of water vapour (with the same absorption as the liquid water), at least for certain wavelengths.

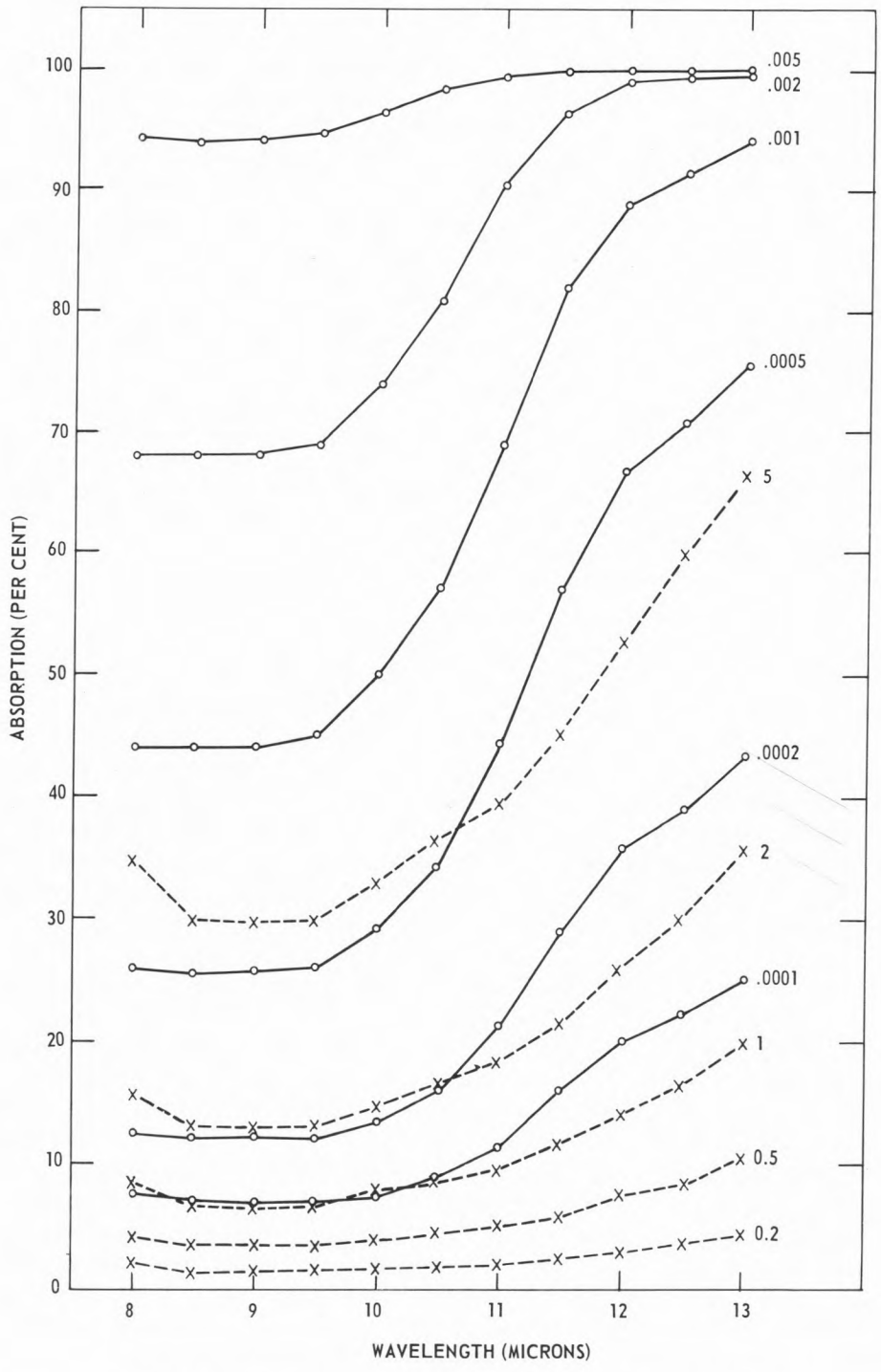

Fig 6 Absorption (percent) by liquid water (solid lines) and water vapour (dashed lines) for wavelengths from 8 to 13 microns, each curve being labelled with the number of precipitable centimetres (x) of water.

It is suggested in Fig 6 that 1 precipitable centimetre (prec cm) of water vapour is the approximate absorptive equivalent of 0.0001 cm of liquid water in the window region. The average of the ratio of the absorption coefficient $k_\ell(\lambda)$ for the wavelengths from 8 to 13 microns is $(1.0 \pm 0.3) \times 10^4$

$$ie, \quad k_\ell(\lambda) = 10^4 k_v(\lambda) \qquad \ldots 15$$

If the amount of liquid water in the air may be measured, we may equate this amount with a corresponding absorptive equivalent of water vapour and thus include water aerosols in radiation chart calculations. Some limitations of this technique will now be discussed, in particular the effects of aerosol scatter, the size distribution and the refractive index variation with relative humidity.

For the range of wavelengths and particle sizes being considered, most of the scattering from aerosols is in the forward direction within a cone of 30^o. Thus although the radiation is scattered slightly, the small amount of radiation backscattered is not regarded as significant compared to the radiation absorbed by aerosol and then reradiated.

The variation of the size distribution within the expected range of the Junge distribution (Eq 3) will not change the scattered radiation pattern sufficiently to alter the above conclusion. The size distribution will also affect the absorptive properties of the cloud. However it can be shown that for an aerosol distribution with particle radii mostly less than 10 microns and for radiation in the atmospheric window region *ie*, $\propto \leqslant 8$, the aerosol absorptive properties may be calculated approximately from consideration of the total mass of aerosol per unit volume rather than by summing the individual particle cross sections using Mie theory (Herman, 1962). Some typical aerosol scattering cross-sections calculated by Mie theory for various infrared wavelengths and relative humidities are discussed in Hoy (1971). Where a significant number of aerosols have radii greater than 10 microns *eg*, in certain fogs or clouds, we find the absorption calculated from the total aerosol mass density overestimates the true absorption calculated from Mie theory. Thus, for the study of aerosol radiative effects prior to fog formation a knowledge of the mass density of aerosol and liquid water is sufficient. This quantity

could be obtained by measuring the aerosol size distribution and summing to obtain the total mass density or by a bulk measurement technique such as measuring the radiation in the atmospheric window which would originate primarily from solid or liquid particles in the air.

The relative humidity of the air will determine how accurately the radiative properties of aerosols may be represented by an equivalent quantity of water vapour. The result of Guttler (1952) together with the growth laws for aerosols of Winkler (1969) suggest that, for a relative humidity between 70% and 80% depending on the composition of aerosol, we may consider the aerosol radiative properties to be very similar to those of liquid water spheres. As relative humidity increases, this equivalence will improve. For relative humidities less than 70%, n_i for liquid water at 10 microns wavelength is 0.05 whereas the assumed n_i for dry aerosol or carbon particles is considerably greater at 0.1 or 0.5 respectively, thus assuming water properties for the aerosol would underestimate their radiative activity. The similarity shown in Fig 6 between water and water vapour absorption would not apply between aerosols with the above n_i values and water vapour. Since the wavelength dependence of aerosol absorption will vary considerably with aerosol type, we may not draw any definite conclusion.

Equation 15 is valid over the wavelength range 8 to 13 microns. Consideration must be given to the change in radiative fluxes resulting from the increase in water vapour concentrations when using Eq 15 for the wavelengths from 4 to 8 and 14 to 30 microns. Most of the radiative flux at the ground, emitted by the atmosphere is of these wavelengths.

For wavelengths less than 9 microns, Eq 15 overestimates the contribution made by the liquid water by several orders of magnitude causing these to be regarded as almost black bodies. However since as little as 0.1 g cm^{-2} of water vapour absorbs almost totally between 5.5 and 7.5 microns, this region may be regarded as a black body and the radiant flux will be only slightly increased. There is some water vapour emission for wavelengths less than 5.5 microns and so the black body assumption here will increase fluxes. However only a very small increase is possible because the black body fluxes here are less than 1% of total fluxes at terrestrial temperatures.

For wavelengths from 13 to 20 microns, the ratio $k_\ell(\lambda)/k_v(\lambda)$ varies from $10^{+4.5}$ to $10^{+3.5}$ using values of $k_v(\lambda)$ from Elsasser and Culbertson (1960) or from $10^{+4.1}$ to $10^{+3.3}$ using values of $k_v(\lambda)$ from Bignell (1970). The region of the spectrum from 14 to 16 microns is normally regarded as black because of strong carbon dioxi e emissions and so any additional radiation due to increased water vapour from Eq 15 will have little effect. The region 16 to 20 microns is almost black for u = 1 cm of H_2O however it is far from black for u = 0.1 cm. The application of Eq 15 should give fairly accurate results in this region because the above ratio of $k_\ell(\lambda)/K_v(\lambda)$ differs only slightly from 10^4. For wavelengths from 20 to 25 microns application of Eq 15 will overestimate the atmospheric fluxes as $k_\ell(\lambda)/k_v(\lambda) \approx 10^3$. This will be most serious for values of $\lesssim$ 0.1 cm. Beyond 25 microns black body fluxes are small and for u = 0.1 cm, water vapour is considered black.

Thus we may expect the application of Eq 15 to enable calculation of increased fluxes from liquid water in the window region fairly accurately where u is the order of 1 cm. For u of the order of 0.1 cm the increased fluxes are less accurate and are at wavelengths beyond 16 microns as well as in the window region. The application of Eq 15 to aerosol studies is best for relative humidities greater than 70% but could produce an order of magnitude result at lower humidities. Thus the tendency for radiation chart calculations to underestimate measured black body radiation fluxes under certain conditions could be at least partially corrected by inclusion of water aerosols as an equivalent amount of water vapour.

Factors Affecting the Accuracy of Radiative Flux Calculations

The accuracy of radiative flux calculations depends to a considerable extent on the accuracy of the absorption coefficients for the atmospheric water vapour and carbon dioxide. The carbon dioxide absorption coefficients are well established as are the water vapour values for the 6 micron band. The values for water vapour absorption for the rotation band beyond about 15 microns are not so well established but there seems reasonable agreement from the few measurements performed. The absorption in the region from about 8 to 13 microns, known as the atmospheric window where absorption is very small, is not well established. This is due to conflicting measurements of its magnitude and the corresponding lack of an adequate theoretical model. Elsasser and Culbertson (1960) mention this problem and adopted the values shown in Fig 5. Bignell (1970) has performed laboratory measurements in this region and his

mean values are given as triangles in Fig 5. He also found that the absorption coefficient was dependent on the vapour pressure of water vapour. Myer (1966) has used different and larger values (crosses in Fig 5) based on work by Yamamoto. Platt (1972) gave a summary of determinations of $k_v(\lambda)$ not included by Bignell which lie between those of Myer and Bignell. Platt was also able to confirm some dependence of water vapour absorption coefficient on vapour pressure from atmospheric measurements over the sea off the Queensland coast. The lack of agreement for values of $k_v(\lambda)$ in the window region limits the accuracy of radiation flux calculation in the atmosphere where the fluxes due to the window region are important, *ie*, for quantities of water vapour greater than about 0.5 prec cm. For smaller quantities of water vapour Elsasser's treatment should be adequate since fluxes in the window region are negligible compared to those from the main bands of water vapour and carbon dioxide.

These uncertainties still ignore the possible effects of aerosols which we have seen may have considerable absorption coefficients. Their effect will be most apparent in the window region and would have contributed to some of the variability in measurements of atmospheric absorption in this region. Carlon (1971), from measurements of the radiative emissions of steam in the atmospheric window region (7 to 14 microns), has derived the following expression for the emissivity ε_λ of an atmosphere containing water vapour and water particles:

$$\ell n \frac{1}{1-\varepsilon_\lambda} = u\left[n k_\ell(\lambda) + (1-n) k_v(\lambda) \right] \qquad \ldots 16$$

where u is the number of precipitable centimetres of water vapour, $k_\ell(\lambda)$ and $k_v(\lambda)$ are the absorption coefficients (cm^{-1}) of liquid water and water vapour and n is the fraction of the total atmospheric water in liquid form.

In order to illustrate the magnitude of effects being considered a simple calculation was performed for 1 km of an isothermal atmosphere with u' = 1.0 prec cm and a temperature of $300^{\circ}K$. The water vapour flux for such an atmosphere from Elsasser (1942) is 0.39 cal cm^{-2} min^{-1}. The

flux from the 8 to 14 micron region using Eq 16 is 0.01 cal $cm^{-2}min^{-1}$ using $k_v(\lambda)$ from Elsasser and Culbertson (1960) 0.03 cal $cm^{-2}min^{-1}$. using $k_v(\lambda)$ from Bignell (1970) and 0.06 cal cm^{-2} min^{-1} using $k_v(\lambda)$ from Bignell and including n = 0.0001 of liquid water. Thus the variation in fluxes using differing $k_v(\lambda)$ in the window region is as great as the variation due to liquid water and this is about 10% of the flux due to the rest of the spectrum. Under these conditions n = 0.0001 corresponds to 10^3 μgm^{-3} of liquid water. This density of water aerosol could occur for unpolluted continental air only at relative humidities greater than 98%, thus it could only assist fog formation in its final stages by an increase in the cooling rate. This density of aerosol could also occur in polluted air trapped under a subsidence inversion for relative humidities of 70% to 80%, thus cooling rates could be expected to increase noticeably, even before the atmosphere is close to saturation.

Lowering the temperature reduces the ability of the air to hold water vapour and so the relative importance of aerosol radiative effects will increase as they are dependent on relative rather than absolute humidity. Thus if aerosols are capable of increasing radiative fluxes by about 10% at $300^{o}K$, at lower temperatures, although the absolute flux increase may be less, the percentage increase will be greater. Radiative cooling is usually almost balanced by eddy transport of heat down the temperature gradient. Thus a sudden change in radiative cooling rate by 10% without the corresponding change in eddy transport could cause rapid loss of temperature over a short time. This assumes some vertical inhomogeneity of either aerosols or humidity profiles so that the radiant energy is transferred to a higher level in the atmosphere. The effect of including water aerosols with n = 0.0001 in atmospheres with varying water vapour content is shown in Table 4. Column 2 gives the flux increase due to water aerosol calculated from Eq 15 using $k_v(\lambda)$ after Bignell (1970) and $k_\ell(\lambda)$ after Irvine and Pollack (1968). Column 3 gives the increase due to aerosols using the procedure previously outlined. For u' = 0.1 and 0.4, the larger column 3 values reflect increased fluxes from 6 to 7 micron and greater than 15 micron regions rather than the window region. The difference between columns 2 and 3 for u' = 4 reflects the inadequate representation of $k_v(\lambda)$ in Elsasser (1942) chart for the window where the increased emission is expected to occur.

Table 4 The increased flux (in cal cm^{-2} min^{-1}) is shown when n = 0.0001 of liquid water aerosol is included in an atmosphere of the given amount u' of water vapour. Column 2 gives the flux increase calculated from Eq 15 and column 3 gives the flux increase calculated using empirical inclusion of liquid water

u' (g cm^{-2})	Flux Increase Using Eq 15	Flux Increase Using Empirical Inclusion of Liquid Water
0.1	0.0031	0.035
0.4	0.012	0.033
1.0	0.025	0.029
4.0	0.053	0.028

Myer (1966) has developed a computer method for calculating radiative fluxes based on the theory of Elsasser and Culbertson (1960). It should be noted that his values of $k_v(\lambda)$ in the window region are larger than Elsasser's adopted values (see Fig 5). Myer (1966) showed two measured spectral intensity curves (plotted against wave number) and, for comparison, his own computed values. The agreement is good except in the window region where the observed values are greater than the computed values, even using his rather high values of $k_v(\lambda)$. Reducing $k_v(\lambda)$, as is required from the observations quoted in Bignell (1970) and Platt (1972), would further increase this difference. Thus it may be seen that radiation calculations considering only the effects of water vapour in the atmosphere are not sufficient for treating radiation in the 8 to 13 micron region of the spectrum and that, where significant radiation occurs in the window region, the fluxes based on water vapour alone may be too low by up to about 10%.

DISCUSSION

Atmospheric Radiation Fluxes from Aerosols

The accurate calculation of radiation fluxes from atmospheric water vapour is restricted by the uncertainty in $k_\nu(\lambda)$ in the 8 to 13 micron region. The Elsasser (1942) chart in particular underestimates radiation from this region for water vapour amount of about 1.0 cm or greater. This chart could be revised using the data of Bignell (1970). The values employed by Myer (1966) seem to be too large in the window region. A computerised computation scheme for calculating radiative fluxes similar to Myer (1966) or Staley and Jurica (1972) is required to correct the errors inherent in the Elsasser chart. A revision of flux emissivities of carbon dioxide, water vapour and ozone are given in Staley and Jurica (1970). Staley and Jurica (1972) comment on the lack of decisive evidence for radiative fluxes from atmospheric aerosols pointing out that the difference between computed and measured radiation fluxes are the same order of magnitude as the possible errors arising from radiometer measurements and uncertainties in $k_\nu(\lambda)$. However most results show that calculated fluxes are systematically less than measured fluxes, their results showing a mean emissivity (ε) excess of 0.03 due to aerosols and/or "unknown trace gases". For $T = 290^{\circ}K$, $\sigma T^4 \doteqdot 0.6$ cal cm^{-2} min^{-1}, the excess flux corresponding to $\varepsilon = 0.03$ is about 0.01 cal cm^{-2} min^{-1} which is of a similar order of magnitude to the values calculated previously.

Preliminary results from a study by Peterson *et al* (1972), who are comparing atmospheric turbidity and aerosol scattering coefficient with hemispheric long-wave radiation at the ground from the atmosphere, show that aerosol concentrations whose scattering coefficient for visible radiation (effective wavelength 0.55 microns) is 0.1 km^{-1} produce a long-wave flux increase at the ground of 0.02 cal cm^{-2} min^{-1}. This scattering coefficient of 0.1 km^{-1} corresponds to an atmosphere with visibility of about 40 km and a mass concentration of aerosol of about 40 $\mu g\, m^{-3}$ (Charlson and Ahlquist, 1969) typical of unpolluted aerosol concentrations. Staley and Jurica (1972) suggest that because visibilities exceeded 30 mi (48 km), the excess emissivity was unlikely to originate from aerosols whereas the work of Peterson *et al* (1972) suggests that aerosols are a likely explanation.

Correlations of visibility deduced from scattering coefficients or otherwise and net long-wave radiation are useful to detect a relationship between aerosol mass and radiative fluxes. Such studies are not sufficient for quantitative applications to predict radiative changes from visibility as visibility is dependent on aerosols between 0.1 and 1.0 micron radius whereas long-wave radiation may depend on aerosols from 0.1 to as much as 4.0 microns radius, depending on the Junge index V. Without detailed studies of aerosol size distributions to relate the variability of distributions above and below 1.0 micron radius, forecasting of long-wave radiation variations from visibility is unlikely to be accurate (Knestrick, Cosden and Curcio, 1962).

The effects of aerosols on atmospheric radiation may be included in a radiation chart calculation by the method outlined in empirical inclusion of liquid water in flux calculations. This is most accurate for relative humidities greater than 70% where aerosol radiative properties may be approximated by those of water spheres. For relative humidities less than 70% an order of magnitude answer only could be expected. To treat radiation from aerosols more precisely a computerised computation scheme, as previously recommended, should be developed which includes not only water vapour, carbon dioxide and ozone but also aerosol material. The mass concentration and vertical variation would need to be specified as well as the generalised absorption coefficient for dry aerosol $k_a(\lambda)$ and water spheres $k_v(\lambda)$. Improved values of $k_a(\lambda)$ should be obtained from the work of Volz (1972a,b).

Zdunkowski and Weichel (1971) have considered numerically the effects of aerosols on radiative transfer in the water vapour window under various conditions. They do not consider the change in aerosol size with changing relative humidity and assume the aerosols act as water spheres. They found natural haze altered significantly the downward atmospheri flux but did not alter the net flux greatly except in the case where a dense aerosol layer was trapped beneath a subsidence inversion.

The dependence of $k_v(\lambda)$ on vapour pressure as determined by Bignell (1970) and approximately confirmed by Platt (1972) should be considered as a future correction to radiation chart computations, provided their observations are verified accurately by others. At 15°C and 11 microns wavelength $k_v(\lambda)$ increases from 0.1 to 0.2 for vapour pressure increase from 0 to 15 mb.

Radiation fluxes prior to radiation fog formation

The ability of aerosols to increase radiation fluxes in the atmosphere has already been demonstrated. The increase occurs largely in the atmospheric window region for water vapour amounts > 0.5 cm (Staley and Jurica, 1970) but also in the longer wavelength region of the rotation band beyond about 15 microns. Rodhe (1962) in his study of the effects of turbulence on fog formation considers the principal cooling of the air is by turbulent transport of heat to a radiatively cooled ground and considers only briefly cooling from fog droplets and atmospheric gases in relation to the growth of the upper fog boundary after formation of droplets. His conclusions are restricted by the very few accurate radiation measurements available to him. In a recent experimental study of radiation fluxes prior to fog formation, Funk (1962), concluded that radiative cooling of the air is the principal cooling process immediately before fog formation.

The greatest radiation cooling of the air would occur where layering of aerosol or relative humidity or both occur, allowing maximum radiative transfer of heat to higher layers in the atmosphere. Small scale advection as noted by Funk (1962) or Stewart (1954) could induce this type of layering. In general, rapid variations in the temperature profile are smoothed out by eddy and radiation transfer of heat whereas humidity and aerosol variations are smoothed by eddy transport only. Stewart noted wide variability in his measured humidity profiles. Little is known about the detailed variations of aerosol concentrations for the first 100 m or so of the atmosphere under the type of nocturnal inversion observed prior to fog formation. An experiment similar to Funk (1962) would be useful, including measurements of aerosol size and number at a number of levels up to say 10 m. Comparison with net radiometer readings would enable definite conclusions regarding radiation from aerosols to be drawn. Layering of aerosols is not absolutely necessary for rapid radiation cooling as a layer of high humidity forms in the first few metres above the ground, due solely to radiative cooling of the ground. The radiation increase by aerosols in this layer alone may induce sufficient additional cooling for fog formation to proceed. The actual additional cooling from aerosols may be obtained by inclusion of data from Table 3 into a radiation flux calculation.

The forecasting of fog from standard meteorological variables is still not satisfactory as there are nights during which fog forms which are not distinguishable from the forecast data, from nights when fog fails to form. The forecast based on screen temperature and dew point where light winds and clear skies are predicted is not greatly improved by the inclusion of parameters based on upper air data or soil temperature (Stewart, 1955). Yee and Bates (1969) have used a net radiometer as a useful aid for short-term (< 4 hr) prediction of fog or low stratus at an aerodrome. They look for decreases of about 0.05 cal cm^{-2} min^{-1} in the net radiation loss during the night which they ascribe to increased emission from "condensed moisture which frequently precedes fog formation". Such studies show promise of providing forecasting aids although, without considerable extra instrumentation the reason for the change in flux is difficult to determine.

Further possible factors influencing cooling rates in the lower atmosphere are the detailed soil temperature and water content profiles affecting the soil thermal capacity, albedo and evaporation at the surface. Zdunkowski *et al* (1967) from a numerical solution of the equations of eddy transport and radiative exchange of heat for the boundary layer on a calm night suggests that the thermal properties of the ground surface are most important for predicting nocturnal temperature of the surface layers whilst eddy exchange is less important. Samamori (1970) has developed a numerical model of the soil and atmospheric boundary layers which he applied to the energy balance of the soil surface as a function of soil wetness. A small change in soil wetness leads to a large change in relative humidity in the surface atmospheric layer during the day. Under calm conditions, such a moist layer would encourage the formation of radiation fog by long-wave cooling of the ground and air after sunset.

Radiation fluxes beneath a subsidence inversion

A second case where aerosol radiative fluxes may be important occurs when particulates and gases from industrial sources are trapped beneath a subsidence inversion, associated with a slowly moving or stationary high pressure system. The air beneath such an inversion, typically about a kilometre or so in depth, may accumulate aerosols for several days, causing a reduction in visibility to less than 5 km even for low relative humidities. The usually dry atmosphere above the

inversion allows strong transmission of long-wave radiation from the relatively moist air beneath the inversion layer, resulting in marked cooling of the air nearest the base of the temperature inversion and in reduced cooling at the ground (Staley and Jurica, 1968). Thus aerosols at even 70% or 80% relative humidity could cause a strengthening of the temperature inversion during the night. Zdunkowski and Weichel (1971) have calculated a cooling rate of 18°C/day due to aerosols alone beneath an inversion whereas water vapour alone produced a rate of 6°C/day. The inversion was 500 m thick with visibility of 0.5 km below the inversion. This is an extreme case but shows that cooling due to aerosols may not be ignored.

During the day long-wave cooling from the inversion will continue. Solar radiation will be absorbed by the aerosols and also backscattered to space by the layer. The net effect of these processes is at present not clear due to insufficient knowledge concerning aerosol scattering and absorption coefficients for infrared wavelengths (Atwater, 1971; Mitchell, 1971). Further study of this problem could aid the control of inversion conditions which may be dangerous if the inversion is allowed to strengthen because of the radiative properties of certain pollutants.

ACKNOWLEDGMENTS

The assistance of Dr K.T. Spillane and Mrs Bettye Macnicol in initiating this project and for useful discussions is gratefully acknowledged.

REFERENCES

Atwater, M.A. 1971 The radiation budget for polluted layers of the urban environment. *J.Appl.Met., 10,* 205-214.

Bakhtiyarov, V.G., Foitzik, L., Perelman, A.Y. and Shifrin, K.S. 1966 The inversion of accurate data on the extinction coefficient by the transparency method. *Pageoph, 64,* 204-211.

Best, A.C. 1951 Drop-size distributions in cloud and fog. *Quart.J.Roy.Met.Soc., 77,* 418-426.

Bignell, K.J. 1970 The water vapour infrared continuum. *Quart.J.Roy.Met.Soc., 96,* 390-403.

Bullrich, K. 1964 Scattered radiation in the atmosphere and the natural aerosol. *Advan.Geophys., 10,* 101-261.

Carlon, H.R. 1970 Infrared emission by fine water aerosols and fogs. *Appl.Opt., 9,* 2000-2006.

Carlon, H.R. 1971 Model for infrared emission of water vapour/aerosol mixtures. *Appl.Opt., 10,* 2297-2303.

Charlson, R.J. and Ahlquist, N.C. 1969 Monitoring of atmospheric aerosol parameters with the integrating nephelometer. *J.Air Poll.Cont.Assoc., 19,* 937-942.

Dufour, L. and Defay, R. 1963 *Thermodynamics of clouds.* Academic Press, N.Y.

Eiden, R. 1966 The elliptical polarisation of light scattered by a volume of atmospheric air. *Appl.Opt., 5,* 569-575.

Eiden, R. 1968 Influence of aerosol on the elliptical polarisation of skylight. *WMO Tech.Note 104,* 275-278

Elsasser, W.M. 1942 Heat transfer by infrared radiation in the atmosphere *Harvard Meteor. Studies No. 6,* Harvard Univ. Press

Elsasser, W.M. and Culbertson, M.F. 1960 Atmospheric radiation tables. *Met.Monog. 4,* 1-43.iv. Press

Fletcher, N.H. 1962 *The physics of rain clouds.* Cambridge Univ. Press

Funk, J.P. 1960 Measured radiative flux divergence near the ground at night. *Quart.J.Roy.Met.Soc., 86,* 382-389

Funk, J.P. 1962 Radiative flux divergence in radiation fog. *Quart.J.Roy.Met.Soc., 88,* 233-249

Goody, R.M. 1964 *Atmospheric radiation I, theoretical basis.* Oxford Press.

Guttler, A. 1952 Die Miesche Theorie der Beugung durch dielectrische Kugeln mit absorbierenden Kern. *Ann.Phys., 11,* 65-98

Hanel, G. 1968 The real part of the mean complex refractive index and the mean density of samples of atmospheric aerosol particles. *Tellus, 20,* 371-379

Harris, F.S. 1969 Particle characteristics from light scattering measurements. *Tellus, 21,* 223-229

Heard, M.J. and Wiffen, R.D. 1969 Electron microscopy of natural aerosols and the identification of particulate ammonium sulphate. *Atmos.Environ., 3,* 355-372

Herman, B.M. 1962 Infra-red absorption, scattering and total attenuation cross-sections for water spheres. *Quart.J.Roy.Met. Soc., 88,* 143-150

Hoy, R.D. 1971 The contribution of the atmospheric aerosol to long wave radiation transfer prior to fog formation. *Proc. Intern.Conf. Weather Modification Canberra, Australia,* 277-281

Irvine, W.M. and Pollack, J.B. 1968 Infra-red optical properties of water and ice spheres. *Icarus, 8,* 324-360

Junge, C.E. 1958 Atmospheric chemistry. *Advan. Geophys. 4,* 1

Junge, C.E. 1963 *Air chemistry and radioactivity.* Academic Press N.Y.

Kasten, F. 1969 Visibility forecast in the phase of precondensation. *Tellus, 21,* 631-635.

Knestrick, G.L., Cosden, T.H. and Curcio, J.A. 1962 Atmospheric scattering coefficients in the visible and infrared regions. *J.Opt.Soc.Amer., 52,* 1010-1016

Kondratyev, K.Y. 1969 *Radiation in the atmosphere.* Academic Press, N.Y.

Kondratyev, K.Y. and Nijlisk, H.J. 1960 Comparison of radiation charts. *Geophys.Pura.Appl., 45,* 231-240.

Maine, R. 1963 Some objective methods of predicting the occurrence of fog conditions. *Sem.aero.f'casting, 3, 2,* Bur.Met.,Australia 1-12.

Mie, G. 1908. Beitrag zur Optik truber Medien. *Ann.Phys., 25,* 377

Mitchell, J.M. 1971 The effect of aerosols on climate with special reference to temperature near the earth's surface. *J.Appl.Met., 10,* 703-714

Myer, V.A. 1966. Infrared radiation from the air to underlying surface. *U.S. Weather Bureau, Technical Note 44-Hydro-1* (unpublished report)

Peterson, J.T., Flowers, E.C. and Singer, I.A. 1972. A study of the effect of atmospheric aerosols on infrared irradiance at the earth's surface. *Preprint Proc. Conf. Atmos. Rad. Ft. Collins, Colorado*

Pittock, A.B. 1968. Seasonal and year to year ozone variations from soundings over south-eastern Australia. *Quart.J.Roy.Met. Soc., 94,* 563-575

Platt, C.M.R. 1972. Airborne infrared radiance (10 to 12 micron wavelength) off tropical east-coast Australia. *J.Geophys. Res., 77,* 1597-1609

Rodhe, B. 1962. The effect of turbulence on fog formation. *Tellus, 14,* 49-86

Sasamori, T. 1970. A numerical study of atmospheric and soil boundary layers. *J.Atmos.Phys., 27,* 1122-1137

Shaw, P. 1963. The physics of fog formation. *Seminar on Aerodrome Forecasting Session 3 paper 1. Bur.Met., Australia.* 1-17

Staley, D.O. and Jurica, G.M. 1968. Radiative modifications of selected vertical temperature distributions. *Quart.J.Roy. Met.Soc., 94,* 310-317

Staley, D.O. and Jurica, G.M. 1970 Flux emissivity tables for water vapour, carbon dioxide and ozone. *J.Appl.Met., 9,* 365-372.

Staley, D.O. and Jurica, G.M. 1972. Atmospheric emissivity under clear skies. *J.Appl.Met., 11,* 349-356

Stephens, J.J. 1961. Spectrally averaged total attenuation scattering and absorption cross-sections for infra-red radiation. *J.Met., 18,* 822-828

Stephens, J.J. and Gerhardt, J.R. 1961. Absorption cross-sections of water drops for infra-red radiation. *J.Met., 18,* 818-822

Stewart, K.H. 1955. Radiation fog: investigations at Cardington, 1951-1954. *M.R.P.912, Met.Res.Cttee, London*

Twitty, J.T. and Weinman, J.A. 1971. Radiative properties of carbonaceous aerosols. *J.Appl.Met., 10,* 725-731

Twomey, S. 1971. The composition of cloud nuclei. *J.Atmos. Sci., 28,* 377-381

Twomey, S. and Howell, H.B. 1967. Some aspects of the optical estimation of microstructure in fog and cloud. *Appl.Opt., 6* 2125-2131

van de Hulst, H.C. 1957. *Light scattering by small particles,* Ed John Wiley, N.Y.

Volz, F.E. 1972a Infrared refractive index of atmospheric aerosol substances. *Appl.Opt., 11,* 755-759

Volz, F.E. 1972b The complex index of refraction from 0.2 to 40 μm. *Preprint Int. Rad. Symp., Sendai, Japan,* May/June

Winkler, P. 1969. Untersuchungen uber das Grossen wachstum naturlicher aerosolteilchen mit der relativen Feuchte nach einer wagen methode. *Annalen der Meteorologie (N.F.), 4,* 134-137

Yamamoto, G. 1952. On a radiation chart. *Sci.Rep. Tohoku Univ., Series 5, Geophys., 4,* 9-23.

Yamamoto, G. and Tanaka, M. 1969. Determination of aerosol size distribution from spectral attenuation measurements. *Appl.Opt., 8,* 447-453.

Yee, L. and Bates, E. 1969. Applications of net radiometer to short range fog and stratus forecasting at Eugene, Oregon. *ESSA Tech.Mem. WR-46*

Zdunkowski, W., Henderson, D. and Hales, J.V. 1967. Prediction of nocturnal temperature changes during a calm night. *Beitr. Phys.Atmos., 40,* 144-157

Zdunkowski, W.G. and Strand, R.F. 1969. Light scattering constants for a water cloud. *Tellus, 74,* 110-133

Zdundowski, W.G. and Korb. 1970. Distribution of radiative energy in ground fog. *Tellus, 22,* 298-317

Zdunkowski, W.G. and Weichel, R.L. 1971. Radiative energy transfer in haze atmospheres. *Beitr.Phys.Atmos., 44,* 53-68

APPENDIX I

AEROSOL VOLUME AND MASS CONCENTRATIONS

To calculate the number of particles per cm^3 for a Junge distribution as in Eq 3, we must integrate over the range of aerosol radii present.

$$dn(r) = 0.434\ c\ r^{-(V+1)}\ dr \quad (cm^{-3})$$

The total number of particles N between radii r_1 and r_2 per cm^3 is given by

$$N = 0.434\ c \int_{r_1}^{r_2} r^{-(V+1)}\ dr$$

$$= \frac{0.434\ c}{V} (r_1^{-V} - r_2^{-V})$$

$$\simeq \frac{0.434\ c}{V}\ r_1^{-V} \qquad \ldots 17$$

where $r_2 >> r_1$. Thus the smallest radius considered determines the total number of particles per cm^3 where $r_2 >> r_1$. For $r_1 = 0.1$ micron, $c = 1$ and $V = 3$, $N \simeq 135$ whereas for $r_1 = 0.05$ micron, $N \simeq 1170$. Adopting $r_1 = 0.1$ microns, the expression for c to ensure the same aerosol number density for all V is

$$c = \frac{V.10^{3-V}}{3}$$

To calculate the volume of particles per cm^3 for a Junge distribution as in Eq 3, we must integrate $\frac{4\pi}{3} r^3\ dn(r)$ over the radii present. The total volume of particles V_o between radii r_1 and r_2 for $V \neq 3$ is given by

$$V_o = \frac{0.434\ c\ 4\pi}{3} \int_{r_1}^{r_2} r^{-V+2}\ dr$$

$$= \frac{1.818\ c}{3-V}\ (r_2^{3-V} - r_1^{3-V}) \qquad \ldots 18$$

where V = 3

$$V_o = \frac{0.434\ c\ 4\pi}{3} \int_{r_1}^{r_2} r^{-1}\ dr$$

$$= 1.818\ c\ \ell n\ \frac{r_2}{r_1} \qquad \ldots 19$$

The volume and mass concentrations of aerosols used in this paper is shown in Table IA. The mass concentrations correspond to those found in unpolluted continental air with the exception of V = 2.5 which is rather large. Typical concentrations found for unpolluted continental air are between 2 and 50 $\mu gm.m^{-3}$ of solid aerosol material.

Table IA The aerosol number density (cm^{-3}), volume concentration (volume of aerosol per 10^6 volumes of air) and mass concentration ($\mu g.m^{-3}$) for aerosol density of 2.0 $g.cm^{-3}$ are shown for the Junge distributions used in this paper, Eq 3 with Eq 9.

V	Number Density (cm^{-3})	Volume Concentration (parts per 10^6)	Mass Concentrations ($\mu g.m^{-3}$)
2.5	135	3.4×10^{-5}	68
3.0	135	9.1×10^{-6}	18
3.5	135	3.9×10^{-6}	7.8
4.0	135	2.4×10^{-6}	4.8